1521-0103/367/1/1–8$35.00
THE JOURNAL OF PHARMACOLOGY AND EXPERIMENTAL THERAPEUTICS

https://doi.org/10.1124/jpet.118.250134
J Pharmacol Exp Ther 367:1–8, October 2018

Role of Interstitial Fluid Turnover on Target Suppression by Therapeutic Biologics Using a Minimal Physiologically Based Pharmacokinetic Model[S]

Xiaobing Li, William J. Jusko, and Yanguang Cao

Department of Pharmacy, Shengjing Hospital of China Medical University, Shenyang, China (X.L.); Division of Pharmacotherapy and Experimental Therapeutics, UNC Eshelman School of Pharmacy, University of North Carolina at Chapel Hill, Chapel Hill, North Carolina (X.L., Y.C.); and Department of Pharmaceutical Sciences, School of Pharmacy and Pharmaceutical, Sciences, State University of New York at Buffalo, Buffalo, New York (W.J.J.)

Received April 23, 2018; accepted July 9, 2018

ABSTRACT

For therapeutic biologics against soluble ligands, the magnitude and duration of target suppression affect their therapeutic efficacy. Many factors have been evaluated in relation to target suppression but the interstitial fluid turnover rate in target tissues has not been considered. Inspired by the fact that etanercept exerts limited efficacy in Crohn's disease despite its high efficacy in rheumatoid arthritis, we developed a minimal physiologically based pharmacokinetic model to investigate the role of the tissue fluid turnover rate on soluble target suppression and assessed the interrelationships between binding constants and tissue fluid turnover. Interstitial fluid turnover rates in target tissues were found to strongly influence target binding kinetics. For tissues with low fluid turnover, stable binders (low k_{off}) exhibit greater target suppression, but efficacy is often restricted by accumulation of the drug-target complex. For tissues with high fluid turnover, fast binders (high k_{on}) are generally favored, but a plateau effect is present for antibodies with low dissociation rates (k_{off}). Etanercept is often regarded as a fast tumor necrosis factor-α (TNF-α) binder (high k_{on}) despite comparable binding affinity (K_D, k_{off}/k_{on}) with adalimumab and infliximab. Crohn's disease largely involves the colon, a tissue with relatively slower fluid turnover than arthritis-associated joint synovium; this may explain why etanercept exerts poor TNF-α suppressive effect in Crohn's disease. This study highlights the importance of tissue interstitial fluid turnover in evaluation of therapeutic antibodies bound to soluble antigens.

Introduction

Several therapeutic biologics that neutralize or block soluble proinflammatory cytokine tumor necrosis factor-α (TNF-α) have demonstrated strong efficacy in the treatment of autoimmune diseases, such as rheumatoid arthritis (RA) and Crohn's disease (CD) (Feldmann et al., 1996; Pizarro and Cominelli, 2007; van Schouwenburg et al., 2013). Monoclonal antibodies (mAbs), such as adalimumab and infliximab and fusion protein etanercept, all exhibit high specificity and affinity for binding to soluble TNF-α and display therapeutic efficacy for RA (Garrison and McDonnell, 1999; Markham and Lamb, 2000; Bang and Keating, 2004). Surprisingly, when using these biologics for CD, another autoimmune disease in which TNF-α is a critical pathogenic factor, only adalimumab and infliximab (but not etanercept) show sufficient efficacy (Olesen et al., 2016). The reason for this difference have focused on the distinct binding affinities of these biologics to transmembrane TNF-α and the role of transmembrane TNF-α in the pathogenesis of CD (Tracey et al., 2008; Horiuchi et al., 2010). Unfortunately, it remains unclear why there is limited efficacy of etanercept in treatment of CD.

For therapeutic biologics that bind to soluble ligands, their efficacy is largely determined by the magnitude and duration of ligand suppression (Wang et al., 2008). According to previous reports (Kim et al., 2007; Song et al., 2008), adalimumab and infliximab have relatively slower association and dissociation rates than etanercept when binding to soluble TNF-α, even though all biologics exhibit comparable binding affinities (K_D) in the subnanomolar range. In addition, compared with etanercept, infliximab and adalimumab frequently form large immune complexes once bound to one or more trimers of soluble TNF-α (Scallon et al., 2002). Such large immune complexes may be responsible for their high risk of tuberculosis (Fallahi-Sichani et al., 2012). For etanercept, such large immune complexes have been seldom reported and the risk of tuberculosis is relatively low (Cantini et al., 2014). There is similar efficacy among the three biologics for RA (Aaltonen et al., 2012). It remains a puzzle why etanercept lacks sufficient efficacy for CD, whereas the other two biologics exhibit strong effect. Here, a modeling approach was used to explore the underlying mechanisms, particularly focusing on

This work was supported by the National Institutes of Health National Institute of General Medical Sciences [Grants R35 GM19661 and R01 GM24211].
https://doi.org/10.1124/jpet.118.250134.
[S] This article has supplemental material available at jpet.aspetjournals.org.

ABBREVIATIONS: CD, Crohn's disease; ISF, interstitial fluid; mAb, monoclonal antibody; mPBPK, minimal physiologically based pharmacokinetic; RA, rheumatoid arthritis; TNF-α, tumor necrosis factor-α.

differences in TNF-α binding kinetics and the role of interstitial fluid (ISF) turnover.

For many antibody-based biologics, the interstitial space within the diseased tissues is their actual sites of action. Tissue ISF is generally believed to be the major extravascular distribution space for antibody-based biologics (Cao et al., 2013; Eigenmann et al., 2017). Vascular convection drives antibody distribution into ISF and then lymphatic drainage provides removal from tissue ISF back into the circulation. The efficiency of lymphatic drainage in target tissues, which essentially determines the ISF turnover rate, is expected to affect antibody-target binding kinetics and binding equilibrium, and might further influence the magnitude and duration of target suppression (Guo et al., 2009; Zhou et al., 2011; Becker et al., 2015). The ISF turnover varies greatly among tissues. For antibodies bound to soluble antigens, evaluating the influence of tissue ISF turnover on target suppression and therapeutic efficacy in disease-associated tissues is warranted.

The second-generation minimal physiologically based pharmacokinetic (mPBPK) model accommodates the fundamental distribution mechanisms of mAbs or fusion proteins, such as lymphatic convection and drainage, and ISF as the primary extravascular distribution space (Cao et al., 2013; Cao and Jusko, 2014b). This modeling approach provides a reasonable approximation of antibody concentrations in ISF, and allows incorporating antibody-target binding kinetics in plasma and/or tissue interstitium, or any other disease-associated tissues (Cao and Jusko, 2014a; Chen et al., 2016, 2017). The present assessment extends the original mPBPK model with a specific disease-associated tissue, where the dynamic ISF turnover was defined. The impact of tissue ISF turnover on TNF-α suppression among three TNF-α antagonists (etanercept, adalimumab, and infliximab) was evaluated to test whether the differences of tissue ISF turnover would explain the limited efficacy of etanercept in CD. Antigen binding kinetics in target tissues for biologics with soluble targets was also explored to test the influence of tissue fluid turnover on target binding kinetics and target suppression. This concept was applied to survey 27 licensed antibodies that bind to soluble ligands for various indications and to evaluate how fluid turnover of their target tissues influenced their efficacy.

Materials and Methods

An Extended mPBPK Model. As shown in Fig. 1, a second-generation mPBPK model is proposed with a specific disease-associated tissue compartment to assess the impact of tissue ISF turnover on the therapeutic efficacy of biologics that bind to soluble antigens. The mPBPK model is described by the following equations:

$$\frac{dC_p}{dt} = \frac{L \cdot C_{lymph} - L_1 \cdot (1-\sigma_1) \cdot C_p - L_2 \cdot (1-\sigma_2) \cdot C_p - C_p \cdot CL_p}{V_p}$$

$$C_p\,(0) = 1000\ \text{nM} \tag{1}$$

$$\frac{dC_{tight}}{dt} = \frac{L_1 \cdot (1-\sigma_1) \cdot C_p - L_1 \cdot (1-\sigma_L) \cdot C_{tight}}{V_{tight}} \tag{2}$$

$$\frac{dC_{leaky}}{dt} = \frac{L_2 \cdot (1-\sigma_2) \cdot C_p - L_2 \cdot (1-\sigma_L) \cdot C_{leaky}}{V_{leaky}} \tag{3}$$

$$\frac{dC_{lymph}}{dt} = \frac{L_1 \cdot (1-\sigma_L) \cdot C_{tight} + L_2 \cdot (1-\sigma_L) \cdot C_{leaky} - L \cdot C_{lymph}}{V_{lymph}} \tag{4}$$

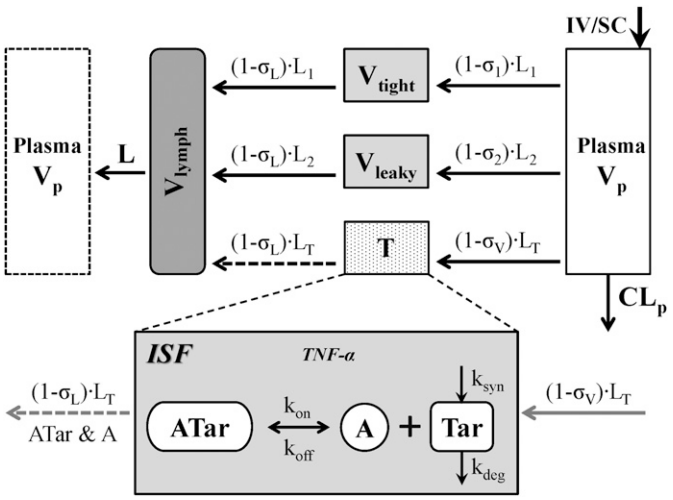

Fig. 1. Second-generation mPBPK model extended with target binding kinetics and ISF turnover in target tissues. The plasma compartment (dashed line) on the left is exactly the same compartment as the plasma compartment on the right. This layout of model structure is consistent with that for full physiologically based pharmacokinetic models. The dashed line of recycled antibody in the target tissue compartment indicates that there is no recycled antibody considered back into the lymph node compartment since the recycled antibody and antibody-target complex account for only a small fraction of total antibody. Symbols are defined in Table 1 and physiologic restrictions are defined in Eqs. 1–7.

where C_p and C_{lymph} are the mAb concentrations in V_p (plasma volume) and V_{lymph} (lymph volume), respectively, in a 70 kg man; C_{tight} and C_{leaky} are the mAb ISF concentrations in two groups of lumped tissues categorized by continuous and fenestrated vascular endothelium structures; and V_{tight} ($0.65 \cdot ISF \cdot K_p$, where ISF is total system ISF and K_p is the available fraction of ISF for distribution) and V_{leaky} ($0.35 \cdot ISF \cdot K_p$) indicate the ISF volumes for tight tissue (muscle, skin, adipose, and brain) and leaky tissue (all other tissues such as liver, kidney, heart, etc.) (Cao et al., 2013). Here, L is the total lymph flow, which is equal to the sum of L_1 (lymph flow for V_{tight}) and L_2 (lymph flow for V_{leaky}), where $L_1 = 0.33 \times$ l and $L_2 = 0.67 \times$ l (Shah and Betts, 2012); σ_1 and σ_2 are the vascular reflection coefficients for V_{tight} and V_{leaky}, which are fixed at 0.95 and 0.71 (Cao and Jusko, 2014b); σ_L is the lymphatic reflection coefficient, which is assumed to be 0.2 in this model (Garg and Balthasar, 2007); and CL_p is the systemic clearance from plasma (Cao and Jusko, 2014b). All initial conditions equal zero except for C_p, which is equal to 1000 nM. In this model, the physiologic parameters (Davies and Morris, 1993) for a 70 kg body weight person are $V_p = 2.6$ l, $V_{lymph} = 5.2$ l, $L = 2.9$ l/day, ISF = 15.6 l, and K_p was set to 0.8 in this case (Wiig et al., 1994; Wiig and Tenstad, 2001). Here, $C_p\,(0) = 1000$ nM was selected within the plasma concentration ranges of many mAbs at their therapeutic doses, which is equivalent to the peak concentrations of antibody in a 70 kg man after being given about 5 mg/kg dose of antibody.

Within the target tissue compartment, the target-mediated drug disposition component was defined for the binding kinetics between biologics and soluble TNF-α. The differential equations are

$$\frac{dA}{dt} = C_p \cdot \frac{L_T}{V_T} \cdot (1-\sigma_V) - A \cdot \frac{L_T}{V_T} \cdot (1-\sigma_L) - k_{on} \cdot A \cdot \text{Tar} + k_{off} \cdot \text{ATar} \tag{5}$$

$$\frac{d\text{Tar}}{dt} = k_{syn} - k_{on} \cdot A \cdot \text{Tar} + k_{off} \cdot \text{ATar} - k_{deg} \cdot \text{Tar} \tag{6}$$

$$\frac{d\text{ATar}}{dt} = k_{on} \cdot A \cdot \text{Tar} - k_{off} \cdot \text{ATar} - \text{ATar} \cdot \frac{L_T}{V_T} \cdot (1-\sigma_L) \tag{7}$$

where A, Tar, and ATar are the concentrations for the antibody, free-target, and antibody-target complex. Parameters k_{on} and k_{off} are the association and dissociation rate constants; k_{syn} and k_{deg} represent the target biosynthesis and degradation rates; and Tar (0) is defined as the target baseline ($= k_{syn}/k_{deg}$). All initial conditions equal zero except for Tar, which equals 100%. The tissue ISF turnover rate was derived from the equation ISF turnover $= L_T/V_T$, where L_T is the lymph flow and V_T is the ISF volume for a target tissue. The values for L_T and V_T are assumed to be 2% of the system lymph flow and 2% of the total ISF volume, respectively. All system parameters employed are listed in Table 1.With the binding parameters of etanercept, we simulated a range of tissue ISF turnover (0.001–100 hour^{-1}), which roughly represented the range of ISF turnover in human tissues. The influence of tissue ISF turnover on concentrations versus time profiles of antibody, free target, and antibody-target complex in target tissues was simulated.

Influence of Tissue ISF Turnover Rate on TNF-α Suppression. The binding kinetic parameters to human soluble TNF-α were obtained from the literature (Kim et al., 2007; Song et al., 2008), where the k_{on} ($\times 10^5$ M^{-1}·s^{-1}) values were 2.59, 0.57, and 1.33 and the k_{off} ($\times 10^{-4}$·s^{-1}) values were 13.1, 1.1, and 0.73 for etanercept, infliximab, and adalimumab, respectively. All target binding parameters are summarized in Table 2.

The area under the target concentrations [Tar(0) − Tar] versus the time curves (Δ area under the curve) for the three TNF-α antagonists were simulated with a range of ISF turnover rates, which covered the ranges for the colon (in CD) and joint synovium (in RA). Since the three biologics have different pharmacokinetics characteristics, degrees of tissue distribution, and approved dosing regimens, it is difficult to accurately predict their target site concentration versus time profiles. Previous pharmacokinetics studies suggested that the three biologics may have similar therapeutic concentrations at their maintenance doses (Tracey et al., 2008). Herein, we assumed average antibody pharmacokinetics and tissue distribution kinetics for three biologics (Table 1). This approximation allowed us to specifically evaluate the influence of tissue fluid turnover rate and binding kinetic constants on target suppression. The role of tissue ISF turnover on TNF-α suppression was compared among the three biologics. The TNF-α suppressive effect in two target-associated tissues, joint synovium and colon, was particularly compared.

Interrelationships between Tissue Fluid Turnover and Target-Binding Constants. For a dynamic range of tissue ISF turnover rates (0.001–100 hour^{-1}), we simulated the influence of increasing k_{on} or decreasing k_{off}, two strategies that could enhance target binding affinity and potentially improve drug efficacy. The impact of binding constants (k_{on} or k_{off}) on tissue accumulation of drug-target complexes was also simulated for a dynamic range of ISF turnover rates.

Survey of Licensed Biologics. In the development of therapeutic antibodies, once a viable target is identified a next step is to decide at which degree of binding affinity the antibody could achieve substantial target inhibition. To better understand the relationships between target binding affinity and ISF turnover rates, we surveyed 27 antibodies that have been approved with soluble targets for many types of diseases. The ISF turnover rates of disease-associated tissues were calculated from the equation L_T/ISF_T, where the L_T and ISF_T values were the lymph flow and ISF volume for specific tissues associated with drug indications collected from the literature (Bauer et al., 1933; Brown et al., 1991; Renkin and Wiig, 1994; Levick, 1998; Shah and Betts, 2012). The biologics adalimumab, belimumab, canakinumab, and infliximab, which have indications associated with multiple indications or tissues, were plotted separately for each indication-corresponding tissue. The ISF turnover rate of tumor is normally low considering the collapsed lymphatic system, which was thus set at 0.0001 hour^{-1}. The values of the average binding affinity for each antibody and the ISF turnover rates of their target-associated tissues are listed in Table 2. The parameter K_a was used (reciprocal of K_d and calculated as k_{on}/k_{off}) to reflect the binding affinity. The target turnover values for each target in Table 2 are listed in Supplemental Table 1.

Simulation and Statistical Analysis. Model simulations were performed using Berkeley Madonna (version 8.3.18; Berkeley Madonna Inc., University of California, Berkeley, CA). All of the graphs and the statistical analysis were performed using GraphPad Prism 6 software (San Diego, CA). The values on the plots are expressed as mean ± S.D.

Results

Influence of Tissue ISF Turnover on Target Binding Kinetics. To evaluate the influence of tissue ISF turnover rate on antibody-target binding kinetics, tissue concentration versus time profiles of antibody, free-target, and antibody-target binding complex for different ISF turnover rates from 0.001 to 100 hour^{-1} were simulated (Fig. 2). When the ISF turnover rate is decreased from 100 to 0.001 hour^{-1}, the amount of antibody that distributes into the target tissues becomes restricted, since lymphatic convection primarily determines antibody access into disease tissues (Fig. 2A). The distribution rate also becomes slower with a decrease in the tissue ISF turnover rate. Tissues with higher ISF turnover rates generally experience stronger target suppression (Fig. 2B), which is partly associated with greater antibody concentrations in these tissues (Fig. 2A). This is also largely ascribed to

TABLE 1
Model parameters employed in the extended mPBPK model simulations

Parameter	Definition	Value	Unit	Reference
σ_1	Vascular reflection coefficient for tight tissue	0.95	—	Cao and Jusko (2014b)
σ_2	Vascular reflection coefficient for leaky tissue	0.71	—	Cao and Jusko (2014b)
σ_L	Lymphatic reflection coefficient	0.20	—	Garg and Balthasar (2007)
σ_V	Vascular reflection coefficient for target tissue	0.50	—	Cao and Jusko (2014a)
L	Total lymph flow	2.9/24	l·h^{-1}	Lindena et al. (1986)
L_1	Lymph flow for tight tissue	0.0399	l·h^{-1}	Shah and Betts (2012)
L_2	Lymph flow for leaky tissue	0.081	l·h^{-1}	Shah and Betts (2012)
CL_p	Systemic clearance	0.01	l·h^{-1}	Cao and Jusko (2014b)
L_T	Lymph flow for target tissue (2% of total)	0.00242	l·h^{-1}	Davies and Morris (1993)
V_{tight}	ISF for tight tissue	8.112	l	Cao and Jusko (2014a)
V_{leaky}	ISF for leaky tissue	4.368	l	Cao and Jusko (2014a)
V_T	ISF for target tissue (2% of total ISF)	0.314	l	Davies and Morris (1993)
V_{lymph}	Lymph volume	5.2	l	Davies and Morris (1993)
V_p	Plasma volume	2.6	l	Davies and Morris (1993)
k_{deg}	Free target degradation rate	4.2	h^{-1}	Cao and Jusko (2014a)
k_{syn}	Target biosynthesis rate in target tissue	4.2	nM·h^{-1}	Cao and Jusko (2014a)

TABLE 2
Properties related to 27 surveyed therapeutic antibodies

Antibody	Average K_D	Target	Target Tissue	ISF Turnover	Reference[a]
	nM			h^{-1}	
Bevacizumab	1.10	VEGF	Tumor	0.0001	Carter (2006)
Romosozumab	0.01	Sclerostin	Bone	0.003	Chouinard et al. (2016)
Eculizumab	0.12	C5	Muscle	0.007	Rother et al. (2007)
Belimumab	0.20	BAFF	Whole body	0.0077	Zhou and Theil (2015)
Ranibizumab	0.046	VEGF	Whole body	0.0077	Platania et al. (2015)
Adalimumab	0.55	TNF-α	Colon	0.04	Song et al. (2008)
Bezlotoxumab	0.75	*Clostridium difficile*	Colon	0.04	Hernandez et al. (2015)
Infliximab	1.92	TNF-α	Colon	0.04	Kim et al. (2007)
Brodalumab	0.239	IL-17RA	Skin	0.05	Greig (2016)
Ixekizumab	0.0018	IL-17A	Skin	0.05	Liu et al. (2016)
Secukinumab	0.166	IL-17A	Skin	0.05	Beerli et al. (2014)
Ustekinumab	0.10	IL-12, IL-23	Skin	0.05	De Luca and Trifonova (2017)
Adalimumab	0.55	TNF-α	Joint synovium	0.15	Song et al. (2008)
Canakinumab	0.031	IL-1β	Joint synovium	0.15	Rondeau et al. (2015)
Certolizumab Pegol	0.09	TNF-α	Joint synovium	0.15	Patel and Moreland (2010)
Etanercept	5.10	TNF-α	Joint synovium	0.15	Kim et al. (2007)
Golimumab	0.018	TNF-α	Joint synovium	0.15	Shealy et al. (2010)
Infliximab	1.92	TNF-α	Joint synovium	0.15	Kim et al. (2007)
Mavrilimumab	0.103	GM-CSF	Joint synovium	0.15	Wang et al. (2018)
Mepolizumab	0.0042	IL-5	Lung	1.21	Hart et al. (2001)
Obiltoxaximab	0.33	*Bacillus anthracis*	Lung	1.21	Nagy et al. (2017)
Omalizumab	0.17	IgE	Lung	1.21	Carter (2006)
Raxibacumab	2.78	Anthrax toxin	Lung	1.21	Mazumdar (2009)
Reslizumab	0.02	IL-5	Lung	1.21	Amini-Vaughan et al. (2012)
Canakinumab	0.031	IL-1β	Kidney	1.46	Rondeau et al. (2015)
Siltuximab	0.034	IL-6	Lymph node	7.91	Deisseroth et al. (2015)
Abciximab	5.00	GPIIb/IIIa	Plasma	58.19	Carter (2006)
Alirocumab	0.58	PCSK9	Plasma	58.19	Poirier and Mayer (2013)
Belimumab	0.2	BAFF	Plasma	58.19	Zhou and Theil (2015)
Evolocumab	0.008	PCSK9	Plasma	58.19	Gibbs et al. (2017)
Idarucizumab	0.002	Dabigatran	Plasma	58.19	Eikelboom et al. (2015)

BAFF, B-cell activating factor; GM-CSF, granulocyte-macrophage colony-stimulating factor; IL, interleukin; VEGF, vascular endothelial growth factor.
[a]The source of the average K_D values for each antibody.

increased efficiency in removing antibody-target complexes from these tissues through fast lymphatic flow; efficient removal of complexes drive target binding kinetics toward complex formation (i.e., association). As shown in Fig. 2C, an antibody-target complex gradually accumulates with a decrease in the ISF turnover rate from 100 to 0.1 hour^{-1}. Greater accumulation of a drug-target complex would disturb the binding equilibrium and drive complex dissociation. Once tissue ISF turnover becomes lower than 0.1 hour^{-1}, the drug-target complex would start to decrease since there would be insufficient tissue antibodies for binding to the target.

Influence of Tissue ISF Turnover Rates on TNF-α Suppression. Compared with infliximab and adalimumab, etanercept is generally regarded as a fast TNF-α binder since it exhibits a higher association rate (k_{on} is 2- to 5-fold higher). In contrast, infliximab and adalimumab are regarded as stable TNF-α binders since they both have relatively lower dissociation rates (k_{off} is much slower than that for etanercept). With such distinct binding kinetics, their TNF-α suppressive effects (Δ area under the curve) in target tissues with changing ISF turnover are shown in Fig. 3. For target tissues with relatively slow ISF turnover rate, i.e., shown on the left-hand side in Fig. 3, infliximab and adalimumab show higher TNF-α suppressive effects. Considering that infliximab and adalimumab are both able to form large immune complexes, their effective dissociation rates are even lower than that at 1:1 binding (Scallon et al., 2002). Thus, the actual TNF-α suppressive effects for infliximab and adalimumab are expected to be greater than what is shown in Fig. 3. Such large immune complexes are seldom observed during etanercept treatment, which would not improve its poor TNF-α suppressive effects in tissue with low fluid turnover. However, along with the increase in tissue ISF turnover, the target suppressive effect of etanercept gradually increases and even surpasses infliximab once the tissue ISF turnover rate is >1 hour^{-1}.

Two target tissues, colon (for CD) and joint synovium (for RA) are shown in Fig. 3 with their reported ISF turnover rates (0.03–0.06 for colon and 0.15–1.0 hour^{-1} for joint synovium). In the colon, two stable binders, infliximab and adalimumab, are expected to exhibit much higher target suppression than the fast binder etanercept. In joint synovium, differences in target suppression become smaller, and etanercept may potentially exhibit even greater TNF-α suppression than infliximab. This simulation provides a theoretical explanation for the limited efficacy of etanercept in CD, even though all three biologics showed comparable efficacy in RA at their therapeutic doses.

Interrelationships between Tissue Fluid Turnover and Target-Binding Constants. Optimization of the target-binding constants (k_{on} and k_{off}) is a critical step in the development of therapeutic antibodies. Here, we simulated the potential effect of altering the target-binding constants on target suppression for tissues with a dynamic range of ISF turnover rates. As shown in Fig. 4A, a gradual increase in k_{on} produces greater target suppression, and there seems to be no capacity limitation in the simulated range, particularly in

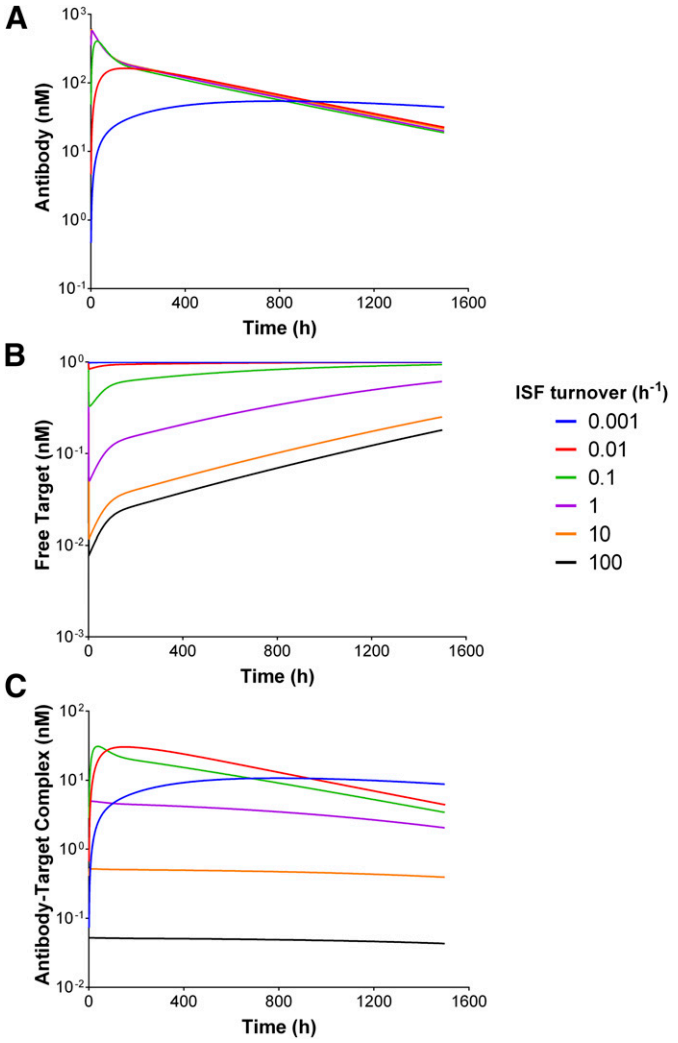

Fig. 2. Simulated target tissue concentration vs. time profiles of free antibody (A), free target (B), and antibody-target binding complex (C) at a dynamic range of tissue ISF turnover rates from 0.001 to 100 hour^{-1}. Tissue ISF turnover rates greatly influence target binding kinetics. Tissues with high fluid turnover are expected to have higher target suppression, which is partly ascribed to increased distribution of antibody and high efficiency in removal of drug-target complexes.

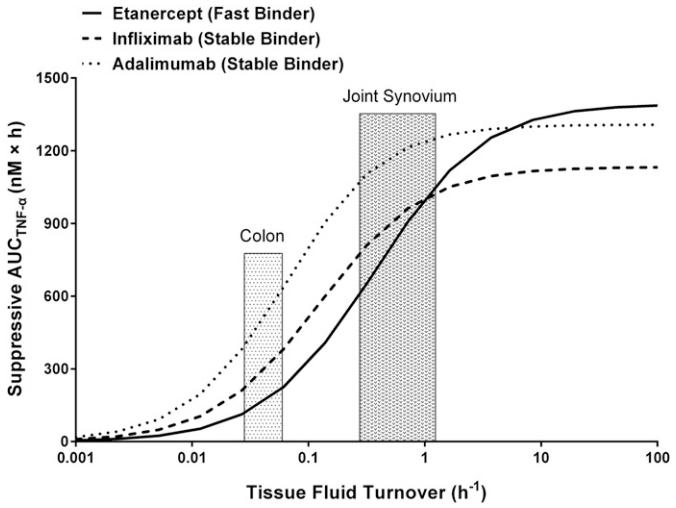

Fig. 3. Simulated interrelationships between tissue fluid turnover rate and the TNF-α suppressive effects [Δ area under the curve (AUC)] by three anti-TNF-α biologics at a dynamic range of tissue ISF turnover rates. Simulation was performed using the binding constants (see Table 1) of each biologic to soluble TNF-α at their therapeutic doses. For joint (in RA), etanercept shows comparable or slightly higher target suppression than adalimumab and infliximab. However, for colon (in CD), etanercept exhibits much less target suppression than the other two biologics.

tissues with higher ISF turnover. On the other hand, a decrease in k_{off} (Fig. 4B), a commonly applied engineering strategy, showed a saturation effect in target suppression. This saturation was particularly apparent in tissues with relatively high ISF turnover rates.

As shown in Fig. 4, C and D, there is considerable accumulation of drug-target complexes in tissues with relatively slow ISF turnover rates. Stronger binding affinity produces increased accumulation of the drug-receptor complex. The increased complex accumulation in tissues with slow ISF turnover rates accounts for their lower target suppression (Fig. 4, A and B).

Four Scenarios Defined by Target Binding Affinity and Tissue ISF Turnover. Considering that the tissue ISF turnover rate and target binding affinity both affect target inhibition, herein we have defined four general scenarios based on the following criteria: high ISF turnover rate (>0.0077 hour^{-1}, the system average) and high target affinity (>1 nM^{-1}); high ISF turnover rate and low target affinity (<1 nM^{-1}); low ISF turnover rate and high target affinity (>1 nM^{-1}); and low ISF turnover rate and low target affinity (<1 nM^{-1}).

These scenarios are shown in Fig. 5A. For tissues with high ISF turnover rates, fast target binders are favored for target inhibition, as indicated in Figs. 3 and 4A. However, there would be a plateau effect at high affinity by lowering k_{off} (Fig. 4B). For tissues with relatively low ISF turnover rates, on average the target suppressive effect would be weaker than for tissues with high ISF turnover rates (Fig. 2B; Fig. 3), where stable binders are generally favored for therapy. Decreasing k_{off} is expected to be more efficacious than increasing k_{on} to improve target suppression in tissues with low ISF turnover rates. However, both strategies encounter the problem of accumulation of drug-target complexes, which could shift the binding equilibrium toward complex dissociation (Fig. 4, C and D). To effectively enhance target suppression for tissues with slow ISF turnover rates, reduction of complex accumulation should be considered as a therapeutic strategy.

Surveyed Licensed Biologics. For the 27 surveyed biologics, the average target binding affinity and the ISF turnover rates of their corresponding disease tissues are summarized in Table 2 and Fig. 5B. Based on the scenarios shown in Fig. 5A, whole body turnover, calculated from the ratio of the total body flow rate and systemic ISF volume (L/ISF = 0.0077 hour^{-1}), is defined as the system average turnover rate and is used to demarcate tissues into two scenarios: low-turnover tissues (tumor, bone, and muscle) and high-turnover tissues (colon, skin, joint, lung, kidney, lymph node, and plasma). As shown in Fig. 5B, 24 out of 27 (~90%) approved biologics are associated with diseases in tissues with high ISF turnover rates. In those tissues with high ISF turnover rates, fast binders with adequate target binding affinities are expected to achieve high target suppression and sufficient therapeutic efficacy. Antibody candidates with fast binding constants thus have a higher possibility of therapeutic success.

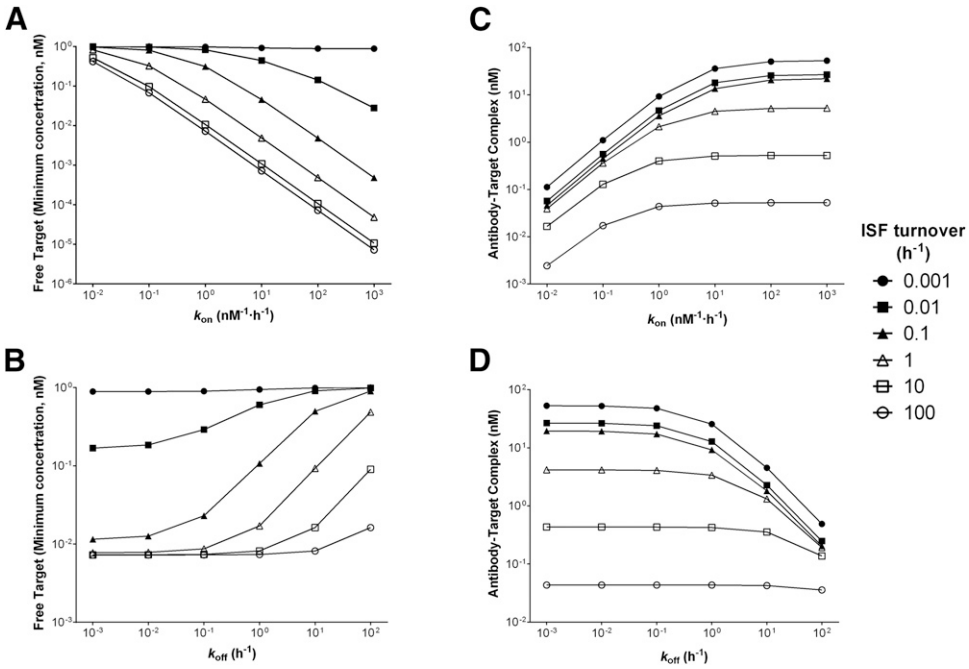

Fig. 4. Influence of changing antibody-target binding kinetics (k_{on} and k_{off}) for a dynamic range of tissue ISF turnover rates on minimum concentrations of free target (A and B) and accumulation of antibody-target complex (C and D). There is a plateau effect by lowering k_{off} to improve binding affinity, particularly for tissues with relatively slow ISF turnover rates.

Discussion

Many therapeutic biologics, such as mAbs and infusion proteins, have been developed to neutralize soluble pathogenic ligands in disease-associated tissues (Wang et al., 2016). For those biologics, the magnitude and duration of target neutralization largely predicts their therapeutic efficacy. Optimization of antibody-target binding constants is an essential strategy to improve therapeutic efficacy (Stein and Ramakrishna, 2017; Tiwari et al., 2017). Inspired by the distinct efficacy of three anti-TNF-α biologics (adalimumab, infliximab, and etanercept) for CD, we used an extended mPBPK model to evaluate the influence of tissue ISF turnover rates on target suppression for biologics that neutralize soluble targets. The different TNF-α suppression effects of the three biologics were simulated at a dynamic range of tissue fluid turnover rates. Even though these biologics exhibit comparable TNF-α binding affinity at the subnanomolar range, adalimumab and infliximab are considered to be stable binders because of their relatively lower k_{on} and k_{off} values to soluble TNF-α compared with etanercept. These two stable binders were predicted to have greater target suppression than etanercept in the CD-site colon. On the other hand, etanercept is expected to have comparable or a slightly stronger TNF-α suppression than adalimumab and infliximab at the RA-site joint synovium. Therefore, the different tissue fluid turnover rates between the colon and joint synovium may explain why etanercept exhibits limited efficacy in CD.

In this study, an mPBPK model with target-mediated drug disposition in a target tissue compartment was developed to demonstrate the importance of tissue fluid turnover rates on the magnitude of target suppression. In the model, tissue degradation of the target-antibody complex was assumed negligible and the antibody-target complex exhibited similar disposition behavior as free antibody (Tiwari et al., 2017). In the developed model, the volume of ISF in the target tissue was assumed to be 2% of the total ISF (with the lymph flow being about 2% of the total lymph flow), which makes the amount of antibody contained in the target tissue not a significant factor in the system mass balance. For simplicity, the recycled antibody was not considered in the plasma compartment. In addition, the Fc-mediated nonspecific clearance pathway was not separately defined in the model since it was included as part of the total linear clearance.

For biologics binding to soluble targets, the ISF turnover rate in disease-associated tissues considerably influenced the magnitude and duration of target suppression. Tissue fluid turnover rates were thus systematically assessed as a critical factor for target suppression. As shown in our analysis, the tissue fluid turnover rate not only determines the tissue concentrations of antibody, but also affects the removal efficiency and accumulation of antibody-target complexes in disease-associated tissue. The latter limits the effect of biologics in suppression of soluble targets. On the other hand, for tissues with relatively fast fluid turnover, a ceiling effect was observed when decreasing dissociation rates beyond target tissue fluid turnover rates in seeking to increase binding affinity and further improve therapeutic efficacy. This concept is summarized in Fig. 5. For example, in the joint synovium, a tissue with fast fluid turnover, a fast binder (high k_{on}) rather than a stable binder (low k_{off}) is favored for improved target suppression. Target suppression cannot be increased when lowering k_{off} beyond the fluid turnover rate. There is no numerical cutoff of k_{on} and k_{off} values for a given antibody to make it a faster or stable binder since it is dependent on the fluid turnover rates in the target tissues. Fast binders should be antibodies that have high k_{on} values to allow the antibody and target to sufficiently bind during the fluid turnover process of their target tissues. Stable binders should be antibodies that have low k_{off} values to keep the antibody-target complex during tissue fluid turnover. These findings have implications for prioritizing strategies in the development of biologics for soluble targets in tissues.

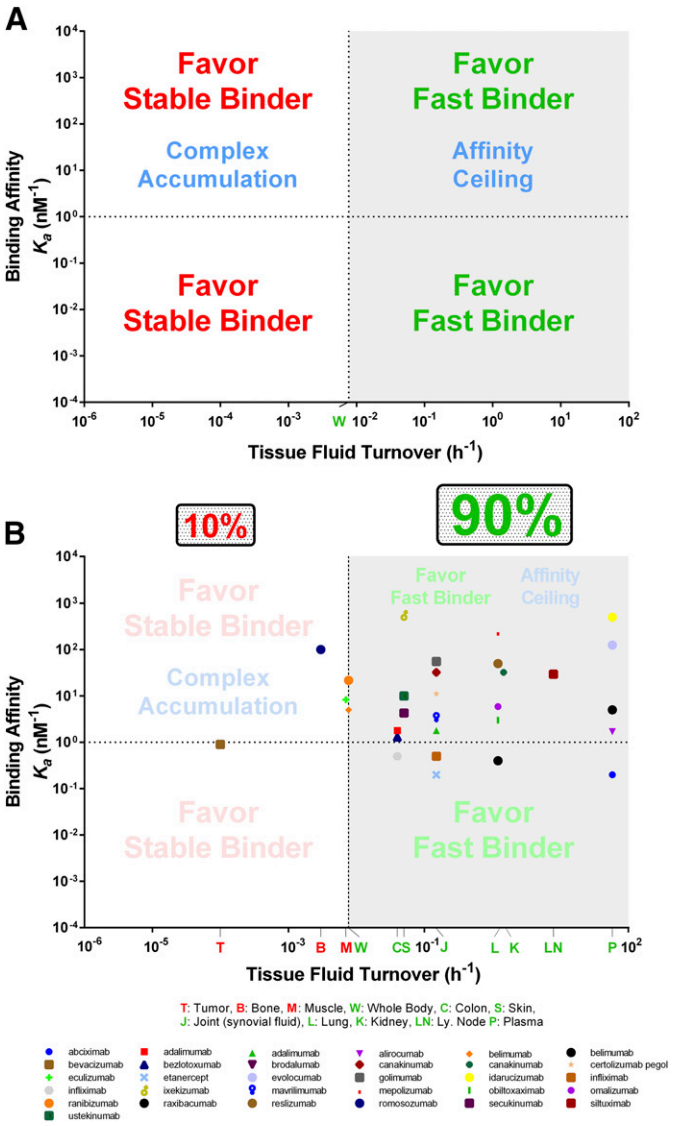

Fig. 5. Four scenarios proposed based on the binding affinity (K_a, = k_{on}/k_{off}) and tissue fluid turnover rate. (A) For tissues with low fluid turnover, stable binders are generally favored but high affinity often confers increased accumulation of antibody-target complex; for tissues with high fluid turnover, fast binders are generally favored but lowering k_{off} beyond fluid turnover rate produces a plateau effect. (B) Summary of 27 licensed antibodies that bind to soluble ligands for treatment of various diseases. Of these, 24 were approved for treatment of diseases that are associated with tissues with relatively high fluid turnover.

Optimization of target binding kinetics to achieve greater binding affinity is the first priority in developing biologics. However, as shown in our analysis, excessive pursuit of high binding affinity is not desirable and even wasteful (Rudnick et al., 2011); selection of sufficient binding affinity while particularly focusing on appropriate binding constants for a given diseased tissue is a rational approach. In surveying the 27 approved biologics with soluble targets, over 90% of the biologics treat diseases associated with tissues having fluid turnover rates higher than the system average. Three exceptions are bevacizumab, romosozumab, and eculizumab. Bevacizumab is an antibody targeting vascular endothelial growth factor, a proangiogenic cytokine used in treatment of multiple types of cancer (colon cancer, lung cancer, glioblastoma, and renal-cell carcinoma). In solid tumors that are generally believed to have low functional lymphatics, bevacizumab-vascular endothelial growth factor complexes are expected to accumulate with lesser therapeutic efficacy (Couzin-Frankel and Ogale, 2011; Van Cutsem et al., 2011; Khasraw et al., 2014). For tissues with relatively slow fluid turnover, strategies to increase lymph flow or enhance local degradation of the drug-target complexes might improve target suppression and efficacy.

Our mPBPK model was used to assess the influence of tissue fluid turnover rate on target suppression for biologics bound to soluble antigens. The simulations help explain why etanercept has limited efficacy in CD. For biologics that bind to soluble antigens in tissues, the interrelationships between target binding constants and tissue fluid turnover rates were also explored, showing that accumulation of drug-target complexes in tissues with slow fluid turnover can restrict the magnitude of target suppression. For tissues with high fluid turnover, a plateau effect was suggested for biologics with low target dissociation rates. These findings may help to prioritize strategies in the development of therapeutic antibodies for various diseases.

Acknowledgments

We thank Dr. Can Liu and Dr. Dongfen Yuan for providing assistance.

Authorship Contributions

Participated in research design: Li, Jusko, Cao.
Conducted experiments: Li, Cao.
Performed data analysis: Li, Cao.
Wrote or contributed to the writing of the manuscript: Li, Jusko, Cao.

References

Aaltonen KJ, Virkki LM, Malmivaara A, Konttinen YT, Nordström DC, and Blom M (2012) Systematic review and meta-analysis of the efficacy and safety of existing TNF blocking agents in treatment of rheumatoid arthritis. *PLoS One* **7**:e30275.
Amini-Vaughan ZJ, Martinez-Moczygemba M, and Huston DP (2012) Therapeutic strategies for harnessing human eosinophils in allergic inflammation, hypereosinophilic disorders, and cancer. *Curr Allergy Asthma Rep* **12**:402–412.
Bang LM and Keating GM (2004) Adalimumab: a review of its use in rheumatoid arthritis. *BioDrugs* **18**:121–139.
Bauer W, Short CL, and Bennett GA (1933) The manner of removal of proteins from normal joints. *J Exp Med* **57**:419–433.
Becker F, Potepalov S, Shehzahdi R, Bernas M, Witte M, Abreo F, Traylor J, Orr WA, Tsunoda I, and Alexander JS (2015) Downregulation of Foxc2 increased susceptibility to experimental colitis: influence of lymphatic drainage function? *Inflamm Bowel Dis* **21**:1282–1296.
Beerli RR, Bauer M, Fritzer A, Rosen LB, Buser RB, Hanner M, Maudrich M, Nebenfuehr M, Toepfer JA, Mangold S, et al. (2014) Mining the human autoantibody repertoire: isolation of potent IL17A-neutralizing monoclonal antibodies from a patient with thymoma. *MAbs* **6**:1608–1620.
Brown TJ, Laurent UB, and Fraser JR (1991) Turnover of hyaluronan in synovial joints: elimination of labelled hyaluronan from the knee joint of the rabbit. *Exp Physiol* **76**:125–134.
Cantini F, Niccoli L, and Goletti D (2014) Adalimumab, etanercept, infliximab, and the risk of tuberculosis: data from clinical trials, national registries, and post-marketing surveillance. *J Rheumatol Suppl* **91**:47–55.
Cao Y, Balthasar JP, and Jusko WJ (2013) Second-generation minimal physiologically-based pharmacokinetic model for monoclonal antibodies. *J Pharmacokinet Pharmacodyn* **40**:597–607.
Cao Y and Jusko WJ (2014a) Incorporating target-mediated drug disposition in a minimal physiologically-based pharmacokinetic model for monoclonal antibodies. *J Pharmacokinet Pharmacodyn* **41**:375–387.
Cao Y and Jusko WJ (2014b) Survey of monoclonal antibody disposition in man utilizing a minimal physiologically-based pharmacokinetic model. *J Pharmacokinet Pharmacodyn* **41**:571–580.
Carter PJ (2006) Potent antibody therapeutics by design. *Nat Rev Immunol* **6**: 343–357.
Chen X, DuBois DC, Almon RR, and Jusko WJ (2017) Interrelationships between infliximab and recombinant tumor necrosis factor-α in plasma using minimal physiologically based pharmacokinetic models. *Drug Metab Dispos* **45**:790–797.
Chen X, Jiang X, Jusko WJ, Zhou H, and Wang W (2016) Minimal physiologically-based pharmacokinetic (mPBPK) model for a monoclonal antibody against interleukin-6

in mice with collagen-induced arthritis. *J Pharmacokinet Pharmacodyn* **43**: 291–304.
Chouinard L, Felx M, Mellal N, Varela A, Mann P, Jolette J, Samadfam R, Smith SY, Locher K, Buntich S, et al. (2016) Carcinogenicity risk assessment of romosozumab: a review of scientific weight-of-evidence and findings in a rat lifetime pharmacology study. *Regul Toxicol Pharmacol* **81**:212–222.
Couzin-Frankel J and Ogale Y (2011) FDA. Once on 'fast track,' avastin now derailed. *Science* **333**:143–144.
Davies B and Morris T (1993) Physiological parameters in laboratory animals and humans. *Pharm Res* **10**:1093–1095.
Deisseroth A, Ko CW, Nie L, Zirkelbach JF, Zhao L, Bullock J, Mehrotra N, Del Valle P, Saber H, Sheth C, et al. (2015) FDA approval: siltuximab for the treatment of patients with multicentric Castleman disease. *Clin Cancer Res* **21**: 950–954.
De Luca C and Trifonova A (2017) Patent disclosure requirements for therapeutic antibody patents. *Expert Opin Ther Pat* **27**:867–875.
Eigenmann MJ, Karlsen TV, Krippendorff BF, Tenstad O, Fronton L, Otteneder MB, and Wiig H (2017) Interstitial IgG antibody pharmacokinetics assessed by combined in vivo- and physiologically-based pharmacokinetic modelling approaches. *J Physiol* **595**:7311–7330.
Eikelboom JW, Quinlan DJ, van Ryn J, and Weitz JI (2015) Idarucizumab: the antidote for reversal of dabigatran. *Circulation* **132**:2412–2422.
Fallahi-Sichani M, Flynn JL, Linderman JJ, and Kirschner DE (2012) Differential risk of tuberculosis reactivation among anti-TNF therapies is due to drug binding kinetics and permeability. *J Immunol* **188**:3169–3178.
Feldmann M, Brennan FM, and Maini RN (1996) Role of cytokines in rheumatoid arthritis. *Annu Rev Immunol* **14**:397–440.
Garg A and Balthasar JP (2007) Physiologically-based pharmacokinetic (PBPK) model to predict IgG tissue kinetics in wild-type and FcRn-knockout mice. *J Pharmacokinet Pharmacodyn* **34**:687–709.
Garrison L and McDonnell ND (1999) Etanercept: therapeutic use in patients with rheumatoid arthritis. *Ann Rheum Dis* **58** (Suppl 1):I65–I69.
Gibbs JP, Doshi S, Kuchimanchi M, Grover A, Emery MG, Dodds MG, Gibbs MA, Somaratne R, Wasserman SM, and Blom D (2017) Impact of target-mediated elimination on the dose and regimen of evolocumab, a human monoclonal antibody against proprotein convertase subtilisin/kexin type 9 (PCSK9). *J Clin Pharmacol* **57**:616–626.
Greig SL (2016) Brodalumab: first global approval. *Drugs* **76**:1403–1412.
Guo R, Zhou Q, Proulx ST, Wood R, Ji RC, Ritchlin CT, Pytowski B, Zhu Z, Wang YJ, Schwarz EM, et al. (2009) Inhibition of lymphangiogenesis and lymphatic drainage via vascular endothelial growth factor receptor 3 blockade increases the severity of inflammation in a mouse model of chronic inflammatory arthritis. *Arthritis Rheum* **60**:2666–2676.
Hart TK, Cook RM, Zia-Amirhosseini P, Minthorn E, Sellers TS, Maleeff BE, Eustis S, Schwartz LW, Tsui P, Appelbaum ER, et al. (2001) Preclinical efficacy and safety of mepolizumab (SB-240563), a humanized monoclonal antibody to IL-5, in cynomolgus monkeys. *J Allergy Clin Immunol* **108**:250–257.
Hernandez LD, Racine F, Xiao L, DiNunzio E, Hairston N, Sheth PR, Murgolo NJ, and Therien AG (2015) Broad coverage of genetically diverse strains of Clostridium difficile by actoxumab and bezlotoxumab predicted by in vitro neutralization and epitope modeling. *Antimicrob Agents Chemother* **59**:1052–1060.
Horiuchi T, Mitoma H, Harashima S, Tsukamoto H, and Shimoda T (2010) Transmembrane TNF-α: structure, function and interaction with anti-TNF agents. *Rheumatology (Oxford)* **49**:1215–1228.
Khasraw M, Ameratunga MS, Grant R, Wheeler H, and Pavlakis N (2014) Antiangiogenic therapy for high-grade glioma. *Cochrane Database Syst Rev* **9**: CD008218.
Kim MS, Lee SH, Song MY, Yoo TH, Lee BK, and Kim YS (2007) Comparative analyses of complex formation and binding sites between human tumor necrosis factor-alpha and its three antagonists elucidate their different neutralizing mechanisms. *J Mol Biol* **374**:1374–1388.
Levick JR (1998) A method for estimating macromolecular reflection by human synovium, using measurements of intra-articular half lives. *Ann Rheum Dis* **57**: 339–344.
Lindena J, Küpper W, and Trautschold I (1986) Catalytic enzyme activity concentration in thoracic duct, liver, and intestinal lymph of the dog, the rabbit, the rat and the mouse. Approach to a quantitative diagnostic enzymology, II. Communication. *J Clin Chem Clin Biochem* **24**:19–33.
Liu L, Lu J, Allan BW, Tang Y, Tetreault J, Chow CK, Barmettler B, Nelson J, Bina H, Huang L, et al. (2016) Generation and characterization of ixekizumab, a humanized monoclonal antibody that neutralizes interleukin-17A. *J Inflamm Res* **9**: 39–50.
Markham A and Lamb HM (2000) Infliximab: a review of its use in the management of rheumatoid arthritis. *Drugs* **59**:1341–1359.
Mazumdar S (2009) Raxibacumab. *MAbs* **1**:531–538.
Nagy CF, Mondick J, Serbina N, Casey LS, Carpenter SE, French J, and Guttendorf R (2017) Animal-to-human dose translation of obiltoxaximab for treatment of inhalational anthrax under the US FDA animal rule. *Clin Transl Sci* **10**:12–19.
Olesen CM, Coskun M, Peyrin-Biroulet L, and Nielsen OH (2016) Mechanisms behind efficacy of tumor necrosis factor inhibitors in inflammatory bowel diseases. *Pharmacol Ther* **159**:110–119.
Patel AM and Moreland LW (2010) Certolizumab pegol: a new biologic targeting rheumatoid arthritis. *Expert Rev Clin Immunol* **6**:855–866.
Pizarro TT and Cominelli F (2007) Cytokine therapy for Crohn's disease: advances in translational research. *Annu Rev Med* **58**:433–444.
Platania CBM, Di Paola L, Leggio GM, Romano GL, Drago F, Salomone S, and Bucolo C (2015) Molecular features of interaction between VEGFA and anti-angiogenic drugs used in retinal diseases: a computational approach. *Front Pharmacol* **6**:248.
Poirier S and Mayer G (2013) The biology of PCSK9 from the endoplasmic reticulum to lysosomes: new and emerging therapeutics to control low-density lipoprotein cholesterol. *Drug Des Devel Ther* **7**:1135–1148.
Renkin EM and Wiig H (1994) Limits to steady-state lymph flow rates derived from plasma-to-tissue uptake measurements. *Microvasc Res* **47**:318–328.
Rondeau JM, Ramage P, Zurini M, and Gram H (2015) The molecular mode of action and species specificity of canakinumab, a human monoclonal antibody neutralizing IL-1β. *MAbs* **7**:1151–1160.
Rother RP, Rollins SA, Mojcik CF, Brodsky RA, and Bell L (2007) Discovery and development of the complement inhibitor eculizumab for the treatment of paroxysmal nocturnal hemoglobinuria. *Nat Biotechnol* **25**:1256–1264.
Rudnick SI, Lou J, Shaller CC, Tang Y, Klein-Szanto AJ, Weiner LM, Marks JD, and Adams GP (2011) Influence of affinity and antigen internalization on the uptake and penetration of Anti-HER2 antibodies in solid tumors. *Cancer Res* **71**: 2250–2259.
Scallon B, Cai A, Solowski N, Rosenberg A, Song XY, Shealy D, and Wagner C (2002) Binding and functional comparisons of two types of tumor necrosis factor antagonists. *J Pharmacol Exp Ther* **301**:418–426.
Shah DK and Betts AM (2012) Towards a platform PBPK model to characterize the plasma and tissue disposition of monoclonal antibodies in preclinical species and human. *J Pharmacokinet Pharmacodyn* **39**:67–86.
Shealy DJ, Cai A, Staquet K, Baker A, Lacy ER, Johns L, Vafa O, Gunn G III, Tam S, Sague S, et al. (2010) Characterization of golimumab, a human monoclonal antibody specific for human tumor necrosis factor α. *MAbs* **2**:428–439.
Song MY, Park SK, Kim CS, Yoo TH, Kim B, Kim MS, Kim YS, Kwag WJ, Lee BK, and Baek K (2008) Characterization of a novel anti-human TNF-α murine monoclonal antibody with high binding affinity and neutralizing activity. *Exp Mol Med* **40**:35–42.
Stein AM and Ramakrishna R (2017) AFIR: a dimensionless potency metric for characterizing the activity of monoclonal antibodies. *CPT Pharmacometrics Syst Pharmacol* **6**:258–266.
Tiwari A, Abraham AK, Harrold JM, Zutshi A, and Singh P (2017) Optimal affinity of a monoclonal antibody: guiding principles using mechanistic modeling. *AAPS J* **19**:510–519.
Tracey D, Klareskog L, Sasso EH, Salfeld JG, and Tak PP (2008) Tumor necrosis factor antagonist mechanisms of action: a comprehensive review. *Pharmacol Ther* **117**:244–279.
Van Cutsem E, Lambrechts D, Prenen H, Jain RK, and Carmeliet P (2011) Lessons from the adjuvant bevacizumab trial on colon cancer: what next? *J Clin Oncol* **29**:1–4.
van Schouwenburg PA, Rispens T, and Wolbink GJ (2013) Immunogenicity of anti-TNF biologic therapies for rheumatoid arthritis. *Nat Rev Rheumatol* **9**:164–172.
Wang B, Wu CY, Jin D, Vicini P, and Roskos L (2018) Model-based discovery and development of biopharmaceuticals: a case study of mavrilimumab. *CPT Pharmacometrics Syst Pharmacol* **7**:5–15.
Wang W, McIntosh TS, Jiang X, Doddareddy R, Dell EC, and Zhou H (2016) Deciphering the in vivo performance of a monoclonal antibody to neutralize its soluble target at the site of action in a mouse collagen-induced arthritis model. *Pharm Res* **33**:1040–1049.
Wang W, Wang EQ, and Balthasar JP (2008) Monoclonal antibody pharmacokinetics and pharmacodynamics. *Clin Pharmacol Ther* **84**:548–558.
Wiig H, Kaysen GA, al-Bander HA, De Carlo M, Sibley L, and Renkin EM (1994) Interstitial exclusion of IgG in rat tissues estimated by continuous infusion. *Am J Physiol* **266**:H212–H219.
Wiig H and Tenstad O (2001) Interstitial exclusion of positively and negatively charged IgG in rat skin and muscle. *Am J Physiol Heart Circ Physiol* **280**:H1505–H1512.
Zhou H and Theil FP (2015) ADME and translational pharmacokinetics/pharmacodynamics of therapeutic proteins. *Gut* **60**:774–779.
Zhou Q, Guo R, Wood R, Boyce BF, Liang Q, Wang YJ, Schwarz EM, and Xing L (2011) Vascular endothelial growth factor C attenuates joint damage in chronic inflammatory arthritis by accelerating local lymphatic drainage in mice. *Arthritis Rheum* **63**:2318–2328.

Address correspondence to: Yanguang Cao, Division of Pharmacotherapy and Experimental Therapeutics, 2318 Kerr Hall, UNC Eshelman School of Pharmacy, University of North Carolina at Chapel Hill, Chapel Hill, NC 27599-7569. E-mail: yanguang@unc.edu